Electronic excited state transport and trapping in disordered systems: Picosecond fluorescence mixing, transient grating, and probe pulse experiments

R. J. Dwayne Miller, Marc Pierre,[a] and M. D. Fayer

Department of Chemistry, Stanford University, Stanford, California 94305
(Received 21 September 1982; accepted 28 December 1982)

A detailed experimental examination of the dynamics of energy transport and trapping in two component systems, using rhodamine 6G (R6G) as the donor and malachite green (MG) as the trap in both glycerol and ethanol solvents, is presented. The experiments were performed using fluorescence mixing and ground state recovery techniques providing temporal resolution of ~50 ps. Samples ranging from high trap-low donor concentrations (the Förster limit) to the opposite regime of high donor and low trap concentrations, were studied. These results were compared with no adjustable parameters to the recent theoretical work of Loring, Andersen, and Fayer (LAF). The excellent agreement between theory and experiment over the entire donor-trap concentration range confirms the theoretical results of LAF and yields a comprehensive description of excited-state dynamics in solution. A variety of dynamic properties are calculated using the LAF theory and the measured parameters associated with R6G-MG system.

I. INTRODUCTION

The radiationless transport of electronic excitations in random systems has been actively studied for over 50 years.[1] The understanding of this problem has had important ramifications in other areas of research such as sensitized fluorescence,[2] sensitized photochemistry,[3] solar energy collection,[4] and in the study of the initial light harvesting steps of photosynthesis.[5]

Theoretical problems associated with excited state transport phenomena have both quantum mechanical and statistical mechanical aspects. Förster[6] and subsequent workers[2,7] have accurately related spectroscopic observables to the intermolecular interactions and transfer rate between a pair of molecules imbedded in a high temperature medium. However, it is the interplay of intermolecular interactions among a large number of molecules that determines the nature of excited state transport in solution. In any microscopic volume, there is a fixed spatial arrangement of atoms or molecules which controls the local time evolution of energy transport. A macroscopic solution contains an infinite collection of all possible local environments. Thus, the time resolved observables of energy transport in solution are ensemble averages over an infinite number of dynamic systems.

Förster treated this many-body problem in two important limiting cases. The first, which we will refer to as the Förster limit, involves two component ensembles of donor and trap molecules in the regime of high trap concentration and near zero donor concentration. Since each donor is surrounded by many traps, the excitation probability flows directly from a donor to the traps with no donor–donor transport. This greatly simplified the problem and allowed an exact theoretical solution. The basic applicability of this result to an experimental system investigated on a picosecond time scale was first demonstrated by Rehm and Eisenthal.[8] (They examined the system rhodamine 6G and malachite green in glycerol which will be discussed extensively below.) The second case treated by Förster[6] was the long time behavior of strictly donor–donor transfer. Förster modeled the solution as a periodic array. Using a truncated Taylor series expansion, he obtained a diffusion equation for the excitation probability and an expression for the diffusion constant.

Although the Förster theory is useful within its restrictions, it is not extendable to other concentration regimes. This has been suggested by a recent picosecond study by Millar, Robbins, and Zewail.[9] Many types of systems of experimental interest occur outside the long time or low donor concentration limits. Transport among chromophores in polymer coils and eventual trapping by eximers[10] (e.g., polyvinyl naphthalene), transport and trapping in photosynthetic units,[5] ruby crystals,[11] or concentrated dye solutions,[12] the short time behavior of transport among identical molecules in nonperiodic media,[13] and similar problems involving electron transport,[14] are but a few examples of important current problems requiring a broader understanding of transport phenomena in disordered systems.

In this paper, we present a detailed experimental examination of the dynamics of electronic excited state transport in two component, donor-trap systems. The experiments were performed using a fluorescence mixing technique which provided ~50 ps time resolution. In conjunction, transient grating and probe pulse methods were also employed. Samples ranging in concentration from the Förster limit to the opposite situation (high donor-low trap concentrations), in which multiple donor–donor steps become important, were studied.

By examing full ranges of concentration and using recent theoretical advances,[15] a detailed understanding of the nature of excitation transport in random systems emerges. For example, excited state transport is found to be nondiffusive, i.e., the mean-square-displacement (MSD) of the excitation does not increase linearly in

[a]Permanent address: Laboratoire de Spectrométrie Physique, Université I, 38041 Grenoble, France.

 0021-9606/83/085138-09$2.10

time. In single component systems (donor–donor transport only), the MSD increases faster at short times and asymptotically approaches diffusive behavior at long time. In two-component systems, this is further affected by the traps. Properties such as the decay of excitation probability on the initially excited molecule, the time evolution of excited donor and trap populations, the time dependent MSD, and the asymptotic value of the diffusion constant can be theoretically calculated.

By more fully understanding excited state transport and trapping in a randomly distributed solution system, we have come close to completing a 50 year old task. The insights gained on solution systems should have important influences in other areas such as mixed crystals and polymer excited state dynamics.

II. THEORY

In this paper, we present the results of time resolved donor fluorescence and donor ground state recovery studies using Rhodamine 6G (R6G) as the donor and malachite green (MG) as the trap in both ethanol and glycerol solvents. These results are compared in detail to the recent theoretical work of Loring, Andersen, and Fayer (LAF)[15] on transport and trapping in disordered systems.

In the last several years there has been considerable theoretical progress in the area. Haan and Zwanzig[16] addressed the problem of donor–donor transport in a one-component system using a density expansion technique. Their theory was restricted to low concentration or short times. Gochanour *et al.*[17] expanded upon their work. Using a diagrammatic expansion, they were able to obtain an accurate approximation to the Green function solution of the master equation. The diagrammatic solution, which contains summations of infinite order sets of diagrams, is good at all times and over a wide range of concentrations. It remains well behaved at very high concentrations, although the accuracy of the approximation is reduced. At about the same time, similar results were obtained by Godzik and Jortner,[18(a)] and Klafter and Silbey,[18(b)] using a continuous time random walk formalism.

Loring, Andersen, and Fayer extended the diagrammatic approach of Gochanour *et al.* to two-component systems composed of donors and traps.[15] Again an accurate approximation for the Green function solution to the system's master equation is obtained. The LAF results permit calculation of experimental observables at all times and for any combination of donor and trap concentration. It reproduces the Förster limit results in the regime of very low donor concentration and high trap concentration. It recovers the results of Gochanour *et al.* in the opposite limit, i.e., high donor concentration and zero trap concentration. For intermediate cases the LAF treatment provides an accurate description of transport and trapping in disordered systems. Comparison to the work of Huber,[19] who used a coherent potential approximation to obtain results for a more restricted set of conditions, shows excellent agreement.

In the experiments described below, the time dependent excited donor population is monitored. Thus we need an expression for $G^D(t)$, which is the part of the Green function which gives the time dependent probability of finding an excitation in the donor ensemble, given that an excitation is created in the donor ensemble at $t=0$. At very low donor and trap concentrations, there is no transport and trapping. In more concentrated systems, the decay of $G^D(t)$ will be determined by the transport dynamics which depends on the donor and trap concentrations and the strengths of the donor–donor and donor–trap interactions. The theoretical development of LAF gives an expression for $G^D(t)$ in Fourier and Laplace transform space, i.e., $\hat{G}^D(\mathbf{k},\epsilon)$, where k is the Fourier transform variable associated with distance and ϵ is the Laplace transform variable associated with the time t. The desired result, the $k=0$ limit of $\hat{G}^D(\mathbf{k},\epsilon)$, is given by

$$\hat{G}^D(0,\epsilon)=\frac{[\hat{G}^s(\epsilon)]^2}{\hat{G}^s(\epsilon)-\tilde{\Delta}[0,\hat{G}^s(\epsilon)]}\ , \tag{1}$$

where $\hat{G}^s(\epsilon)$ (a diagrammatic series) is the probability of finding the excitation on the initially excited donor molecule and $\tilde{\Delta}[0,\hat{G}^s(\epsilon)]$ is another diagrammatic series defined in Ref. 15.

Loring, Andersen, and Fayer provide expressions for the two infinite series needed to evaluate Eq. (1). The expression for $G^s(\epsilon)$ is given by

$$[G^s(\epsilon)]^{1/2}=\left[-\left(\frac{\pi}{2\tau_D^{1/2}}\gamma C_T+\frac{\pi}{2^{3/2}\tau_D^{1/2}}\gamma C_D\right)+\left[\left(\frac{\pi}{2\tau_D^{1/2}}\gamma C_T+\frac{\pi}{2^{3/2}\tau_D^{1/2}}\gamma C_D\right)^2+4\left\{\epsilon-\frac{0.34}{\tau_D}\gamma^2C_T^2-\frac{0.19}{\tau_D}\gamma^2C_D^2-(0.14+\beta-\alpha)\frac{\gamma^2}{\tau_D}C_TC_D\right\}\right]^{1/2}\right]\Big/2\left[\epsilon-\frac{0.34}{\tau_D}\gamma^2C_T^2-\frac{0.19}{\tau_D}\gamma^2C_D^2-(0.14+\beta-\alpha)\frac{\gamma^2C_TC_D}{\tau_D}\right]\ , \tag{2}$$

where

$$C_D=\tfrac{4}{3}\pi R_0^{DD^3}\rho_D\ , \tag{3a}$$

and

$$C_T=\tfrac{4}{3}\pi R_0^{DT^3}\rho_T\ . \tag{3b}$$

C_D and C_T are the reduced concentrations and ρ_D and ρ_T are the number densities for donors and traps, respectively. R_0^{DD} (donor–donor) and R_0^{DT} (donor–trap) are lengths which characterize the excited state intermolecular transfer interactions.[6] α and β are functions which depend only on R_0^{DT}/R_0^{DD}. These functions have

been tabulated.[15] γ is an orientation factor which is determined by the angular dependence of the intermolecular interaction. For a dipole–dipole interaction, there are two limiting cases. If the molecules are in fixed random orientations $\gamma = 0.846$. If the molecules are rotating on a time scale rapid relative to the characteristic times involved in the transport $\gamma = 1$. (This factor is discussed in more detail in Sec. IV.) τ_D is the excited state lifetime of the donor in the absence of trapping.

The expression for $\tilde{\Delta}(0, \epsilon)$ is given by

$$\tilde{\Delta}(0,\epsilon) = \frac{\pi}{2\sqrt{2}}\,\gamma C_D\,\tau_D^{-1/2}\,[\hat{G}^s(\epsilon)]^{3/2} + \left(\alpha - 0.1887\,\frac{C_D}{C_T} - 0.3832\right)\gamma^2 C_D C_T\,\frac{[\hat{G}^s(\epsilon)]^2}{\tau_D}\,. \tag{4}$$

The parameters in Eq. (4) are defined above.

Equation (1) with Eqs. (2) and (4) give the expression for $\hat{G}^D(\epsilon)$, the Laplace transform of the probability of finding the excitation in the donor ensemble, i.e., of finding an excitation which has not trapped. This expression does not include loss of donor probability due to decay of the donor to its ground state. To obtain an expression for use in comparison to experiments,[15] first $\hat{G}^D(\epsilon)$ is numerically inverted to give $G^D(t)$. $G^D(t)$ is then multiplied by a decaying exponential to account for the donor excited state lifetime, i.e.,

$$N^D(t) = G^D(t)\,e^{-t/\tau_D}\,, \tag{5}$$

where $N^D(t)$ is the number of excited donor molecules as a function of time. $N^D(t)$ is directly proportional to the time resolved fluorescence decay, the experimental observable in the fluorescence mixing experiments. It is also the observable in the transient grating and probe pulse experiments discussed below.

III. EXPERIMENTAL

Fluorescence mixing, transient grating, and probe pulse techniques were used to study the donor dynamics. All three utilized the same 500 Hz repetition rate acousto-optic, Q-switched, mode-locked, Nd-YAG system, but with different external components. The laser system provides spatially and temporally Gaussian 1.06 μ single pulses (TEM_{00}) with pulse durations of 138 ± 4 ps and energies of ~45 μJ. This single pulse can be converted to produce a 0.532 μ (105 ps) single pulse and/or 0.355 μ (80 ps) single pulse. Shot-to-shot fluctuations were ~3% and long term laser power drift was less than 1%.

The fluorescence mixing experiment is illustrated schematically in Fig. 1. With this technique, the 0.532 μ single pulse is used to excite the sample. The resulting fluorescence is collected by an achromatic lens and focused collinear with the IR single pulse into an RDP type I summing crystal. Only the fluorescence component polarized parallel to (and coincident in time with) the 1.06 μ single pulse sums to produce UV, ~0.390 μ. The intensity of the UV is proportional to the fluorescence at that time. The excitation pulse was polarized at $54.7 \pm 0.5°$ (the magic angle) with respect to the IR single pulse and the RDP crystal axis to eliminate fluorescence depolarization effects arising from molecular rotation[20(a),20(b)] or excited state transport.[13] The donor decay is time-resolved by varying the delay between the 0.532 μ pulse and the 1.06 μ summing pulse with a motorized delay line. The upconverted fluorescence signal is detected, after selectively filtering (Fig. 1), by a cooled photomultiplier (EMI 6256).

EXPERIMENTAL SETUP

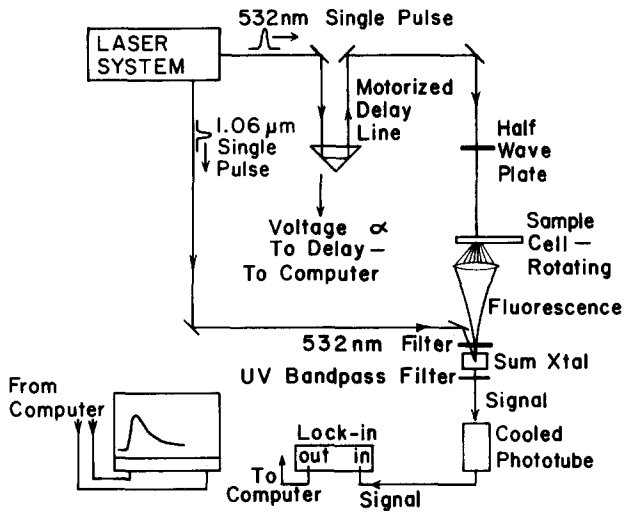

FIG. 1. Time resolved fluorescence mixing experimental set up. The laser system consists of a 500 Hz repetition rate, acoustooptically mode-locked and Q-switch Nd: YAG laser. The sample is excited by a 0.532 μ Nd: YAG second harmonic single pulse. The resulting fluorescence which is time coincident in the summing crystal with a 1.06 μ Nd: YAG fundamental pulse is summed to produce a UV signal pulse which is proportional to the fluorescence at that time. The motorized delay line provides temporal resolution by varying the time between the sample excitation and the fluorescence summing.

Transient grating experiments[21] were performed with both 0.532 and 0.355 μ pulses as excitation. The excitation pulse is beam-split by a 50% reflector, and the resulting two pulses are recombined at an angle in the sample to form an interference pattern. The extent of optical absorption as a function of spatial position mimics the interference pattern. The spatially periodic distribution of excited states acts as a holographic diffraction grating. A 0.532 μ probe pulse, brought in at the appropriate angle for Bragg diffraction, measures the difference in the optical density between the grating peaks and nulls. This is proportional to the excited state population. In this experiment the 0.532 μ probe pulse is variably delayed. The probe pulse was polarized at the magic angle to eliminate depolarization influences on the signal.

Probe pulse experiments were performed in the usual manner[9] with either 0.532 or 0.355 μ excitation pulses and 0.532 μ probe pulses. The excitation beam is chopped at one-half the laser repetition rate, and the

difference in probe pulse transmission is measured as a function of probe pulse delay.

In all experiments, fluorescence mixing, transient grating and probe pulse, the signal from the photodetector was amplified with a lock-in amplifier. The output of the lock-in and voltage proportional to the delay distance (which is proportional to the delay time), were digitized and stored on disk. This facilitated direct comparison of theory and experiment.

The donor, laser grade rhodamine 6G chloride (Pilot Res.), and the trap, malachite green oxalate (Eastman Kodak ~99% pure), were used without further purification. Solutions of R6G and MG were prepared in both spectroscopic ethanol and glycerol (< 0.05% H_2O, Fisher) and used within an hour of preparation. Samples were studied in a rotating cell to avoid heat and photodecomposition problems. The cell thickness was adjustable from 1 to 300 μ. Sample thickness studies were made to ensure that reabsorption did not influence the experimental results. It was found that an optical density of 0.06 or less, at 0.532 μ would eliminate reabsorption problems in the system studied. The intensity of laser excitation was attenuated by a series of neutral density filters until stimulated emission and other power-dependent effects were eliminated. For the focusing parameters used, the excitation intensity was typically less than 2×10^{14} photons/cm^2.

The spectroscopic measurements of R_0^{DD} and R_0^{DT} were determined by the spectral overlap method of Förster.[6] Fluorescence spectra of R6G were recorded and digitized with a computer interfaced Spex 1870 1/2 m monochromator equipped with an EMI 9658 photomultiplier. Corrections were made for the monochromator and photomultiplier tube wavelength response using a blackbody radiation lamp of known color temperature. Disodium fluorescein in H_2O was used as the quantum yield standard[22] (pH = 13) and the excitation wavelength of 0.465 μ (100 Å bandwidth) was isolated by an interference filter from the output of 100 W Xe-arc lamp. Index of refraction effects were taken into account.[23] Absorption spectra of both R6G and MG were recorded with a computer interfaced Cary 14 spectrometer. The digitized absorption and fluorescence data were used to numerically calculate the absorption–emission overlap integral.

In the presence of traps, excited donor decay curves are nonexponential. For finite duration excitation and detection pulses, a detailed comparison of experiment and theory requires that the theoretical function be convolved with known pulse shapes. The necessary convolution integrals for fluorescence mixing, transient grating, and probe pulse experimental techniques have been given previously.[13,24]

IV. RESULTS AND DISCUSSION

The time resolved fluorescence mixing data for a dilute (1×10^{-4} M) ethanol solution of R6G is shown in Fig. 2. This concentration is so low that excited state transport is negligible.[13] The solid curve drawn through the data represents an exponential decay, appropriately convolved with the pulse durations of the 0.532 μ excitation pulse and 1.06 μ summing pulse. From these measurements, the lifetime of R6G is 3.71 ± 0.04 ns. The same results were found for higher concentrations (1×10^{-3} M). The excellent agreement between the convolved calculated curve and the data demonstrates that the fluorescence mixing technique is free of artifacts. Fluorescence depolarization due to molecular rotation and donor–donor energy transport can have dramatic effects on curve shapes.[13,20] The imperceptible deviation from an exponential decay indicates the magic angle, 54.7° between the excitation and detection polarizations, properly eliminates depolarization effects from the data. Figure 2 also serves as a reference measurement of the extent of agreement possible between convolved theoretical decays and experiment.

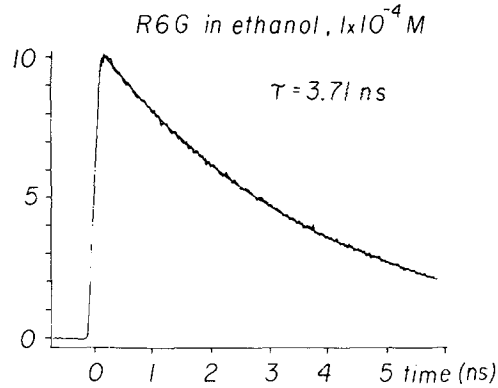

FIG. 2. Time-resolved fluorescence mixing data for a low concentration sample (1×10^{-4} M) of R6G in ethanol. This and data from other low concentration samples yield a lifetime of 3.71 ± 0.04 ns. The solid curve running through the data was calculated by appropriately convolving an exponential decay with the excitation and detection pulse profiles. The agreement at this concentration and at higher concentrations (R6G = 1×10^{-3} M) demonstrate that depolarization effects arising from rotation or donor–donor energy transport have been eliminated by exciting the sample at the magic angle (54.7°). The agreement between the data and the calculated curve also shows that the convolutions are handled accurately and that the experiment is free of artifacts at $t = 0$.

Given τ_D, the only remaining parameters in the LAF theory are R_0^{DT} and R_0^{DD}. These were determined independently from the overlap of the fluorescence and absorption spectra of R6G with MG, and R6G with R6G, as discussed in Sec. III. As a first test of procedures and to confirm the spectroscopic measurements, the Förster limit was studied and R_0^{DT} was obtained. The results of the fluorescence mixing studies are shown in Fig. 3(a). The MG concentrations were varied from 5×10^{-4} M to 3×10^{-3} M with R6G concentrations of 1×10^{-4} M. Higher concentrations of MG than 3×10^{-3} M absorbed almost all the fluorescence, making the signal to noise ratio too low to be useful. The solid lines through the data were obtained by convolving Eq. (5) with the excitation pulse and then convolving this result with the detection pulse at various times in the decay. The reduced donor concentration was $C_D = 0.02$ (no donor–donor transport) and the orientational factor γ was taken to be unity. R_0^{DT} was used as an adjustable param-

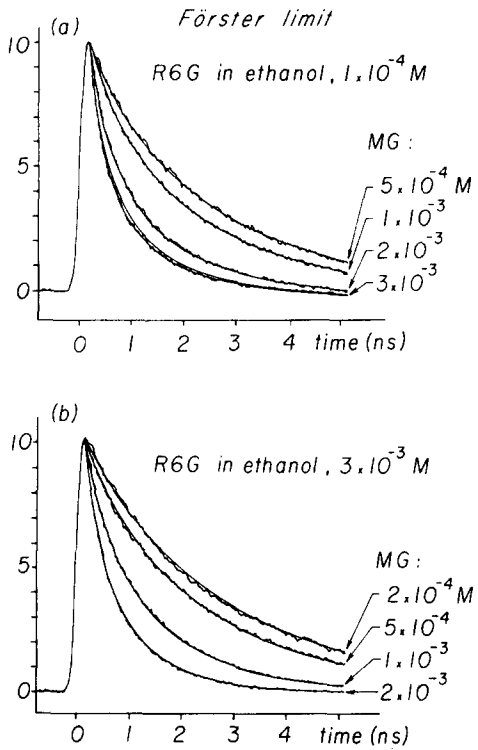

FIG. 3. Time-resolved fluorescence mixing data for R6G-MG ethanol solutions (a) The Förster limit. The R6G concentration is low (1×10^{-4} M) and the MG concentrations (indicated) are high. Only donor to trap energy transport occurs. The solid curves through the data were calculated using R_0^{DT} as an adjustable parameter. For all curves, R_0^{DT} is 58 ± 1 Å. The sensitivity of the calculation to R_0^{DT} is illustrated by the two solid lines for the 3×10^{-3} M data. The upper solid line was calculated with R_0^{DT} = 57 Å while the curve through the data has R_0^{DT} = 58 Å. The time-resolved measurement of R_0^{DT} agrees well with the spectral overlap measurement of 59 ± 1 Å. (b) High donor concentration systems. At this R6G concentration (3×10^{-3}) the effects of donor–donor energy transport become appreciable. This can be seen by comparing the curves in (a) and (b) with the same MG concentration. The solid curves through the data were calculated with the LAF theory without adjustable parameters using the independently determined values of R_0^{DT}, R_0^{DD}, and τ. The agreement between theory and experiment over the MG concentration range studied is excellent.

eter to obtain the calculated curves in Fig. 3(a). All the concentrations were fit with a single value of R_0^{DT} = 58 ± 1 Å. The accuracy of this measurement is demonstrated in Fig. 3(a) for the MG concentration of 3×10^{-3} M. The top solid curve is calculated with an R_0^{DT} of 57 Å while the curve running through the data has an R_0^{DT} of 58 Å. The calculated curve with R_0^{DT} = 59 Å (not shown) is symmetrically displaced from the 58 Å curve. The measurement of R_0^{DT} (= 58 Å) is in excellent agreement with the spectral measurement which found R_0^{DT} = 59 ± 1 Å. The close agreement between the spectroscopically determined value of R_0^{DT} and the time resolved measurements over a wide range of concentrations supports the accuracies of the determinations. It also demonstrates that it is sufficient to describe transport in this system in terms of a dipole–dipole interaction since the spectroscopic measurement gives only the dipole contribution but the time dependent measurement would be influenced by higher multipole terms as well.

The value of R_0^{DT} as reported above is not in close agreement with the value of 52.5 ± 0.5 Å determined by Porter and Tredwell.[25] To check for systematic errors in our time resolved measurements, we repeated the Förster limit concentration studies using transient grating and probe pulse techniques at two different excitation wavelengths, 0.532 and 0.355 μ. The results were very close to those obtained from the fluorescence mixing experiments with the probe pulse and transient grating measuring R_0^{DT} = 57 ± 1 Å and R_0^{DT} = 58 ± 2 Å, respectively. The difference in the Porter and Tredwell results are probably due to reabsorption effects. Porter and Tredwell used samples with path lengths of 200 μ for 10^{-4} M R6G solutions. For the same concentration, we found it necessary to use path lengths of less than 125 μ. The thicker samples gave data which decayed significantly slower than the data obtained in the limit of an optically thin sample. Porter and Tredwell's R6G lifetime measurements of 4.2 ± 0.2 ns also show the effects of reabsorption as it is significantly longer than the 3.71 ns lifetime we obtained with fluorescence mixing experiments. The fluorescence mixing experiments were confirmed by probe pulse and transient grating measurements which measured τ_D = 3.7 ± 0.1 ns and τ_D = 3.65 ± 0.05 ns, respectively.

Figure 3(b) displays fluorescence mixing data for a series of experiments on the general transport and trapping problem in which the donor concentration and donor–donor transport are significant. The curves are for fixed R6G donor concentration. *The solid lines through the data are calculated using Eq.* (5) *with no adjustable parameters.* The following values of the parameters were employed τ_D = 3.71 ns, R_0^{DT} = 58 Å, γ = 1.0, R_0^{DD} = 55 Å, α = 0.244 and β = 0.548. The values of τ_D, R_0^{DT}, and γ are discussed above. R_0^{DD} is taken from recent spectroscopic measurements,[26] and α and β are from those tabulated by LAF. The agreement between experiment and theory is very good. Equally good agreement was obtained for systems in which the R6G concentration was 2×10^{-3} M and 1×10^{-3} M. The effect of donor–donor transport is significant as can be seen by comparing the results in Fig. 3(b) to the Förster limit results having the same MG concentrations. For example, τ_{eff} (the time required for the signal to fall to $1/e$) for 1×10^{-3} MG samples in the Förster limit is ~2 ns [Fig. 3(a)]. The same MG concentration, but with a R6G concentration of 3×10^{-3} M, has a τ_{eff} of ~1.4 ns [Fig. 3(b)].

Trapping by R6G dimers[12] was not accounted for in the calculations. The R6G dimer equilibrium constant is small and corrections to the donor concentration are unnecessary. Even at the lowest MG concentrations the R6G dimer concentration is not significant. This is supported by the agreement between experiment and theory for a variety of R6G concentrations.

The experiments described above demonstrate that the LAF theory is able to account for donor–donor energy transport and trapping in solution for moderately

high donor concentrations, i.e., $C_D = 1$. Higher concentrations could not be studied using the fluorescence mixing technique as the sample cell could not be made thin enough to avoid reabsorption problems.

In order to extend the donor concentration range, we used the transient grating technique. While the distance scale associated with reabsorption problems in fluorescence mixing or probe pulse experiments is on the order of the laser spot size, in a transient grating experiment, the distance is on the order of the interference fringe spacing (~1 μ). This decrease in length greatly reduces the influence of reabsorption on transient grating measurements. However, there is one drawback in using the transient grating method in EtOH solutions. The transient grating excitation generates acoustic waves in addition to electronic excitations. The laser induced acoustic waves imposed a 5% sinusoidal modulation on the signal. This effect has been well characterized.[27] Despite the laser induced acoustic waves, transient grating studies showed excellent agreement with the LAF theory. The theory correctly predicted the curve shapes up to the highest donor concentration studied ($C_D \sim 3$) and over the entire MG concentration range ($2 \times 10^{-3} - 2 \times 10^{-4}$ M).

There are two possible additional factors associated with a low viscosity solvent such as EtOH that need addressing, although their net effect on these experiments is negligible. Several authors have predicted that physical bulk diffusion of the donor and trap molecules through the solution can influence the excited state dynamics in the Förster limit[28] and presumably at higher donor concentrations as well. Also R6G and MG do not rotate at a fast enough rate compared to the transport rates to completely justify the use of the angle averaged interaction strength, i.e., the orientational factor should be somewhat less than unity; $\gamma < 1$.

In these experiments, no hint of bulk diffusion effects could be detected. The Förster limit yielded a consistent R_0^{DT}, within 1 Å over the range of concentrations studied. Bulk diffusion effects should manifest themselves most clearly as deviations from the predicted concentration and time dependence. However, as Fig. 3(a) illustrates, the agreement is near perfect for all concentrations. Recently, it has been reported[9] that there are significant diffusion effects in systems involving azulene, a small molecule, as the trap in MeOH. The diffusion constant for azulene, assuming a Stokes–Einstein relation[25,29] is much larger than MG or R6G. In ethylene glycol where the azulene diffusion length l to R_0 ratio is the same as for MG with R6G in EtOH ($l/R_0 \sim 1/3$), bulk diffusion effects were undetectable. It is therefore reasonable to conclude that for the systems studied here, the effect of the small amount of bulk molecular diffusion of donor and trap molecules is negligible.

The orientational factor γ has been treated by Bojarski and Dudkiewicz[30] for the regime intermediate between rapidly rotating molecules and static molecules. From this work and the known rotation times of R6G and MG,[20(a),25] γ should be ~0.95. The difference between the true γ factor and the γ for free rotation has been absorbed in the time-resolved R_0^{DT} determinations. Therefore, the discrepancy between the actual γ factor and unity is of no consequence for R_0^{DT} and will be within experimental error for R_0^{DD}. In fact, if the value predicted by the theory of Bojarski and Dudkiewicz is used, R_0^{DT} becomes 59 Å which is in better agreement with the spectral determination of R_0^{DT}.

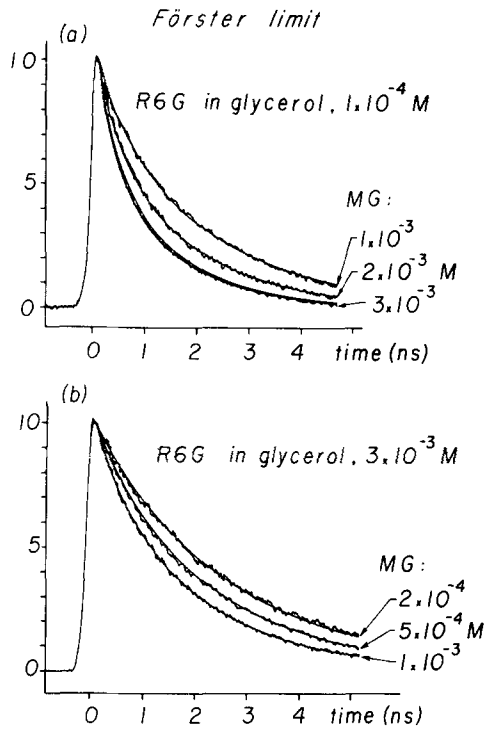

FIG. 4. Time-resolved fluorescence mixing results for R6G-MG glycerol solutions. (a) The Förster limit. The solid curves through the data were calculated as in Fig. 3a with $\tau_D = 3.17$ and $\gamma = 0.846$. R_0^{DT} was determined to be 54 ± 1 Å. The sensitivity of the determination is shown by the two curves for the 3×10^{-3} M MG data. The upper curve is for $R_0^{DT} = 53$ Å and the lower curve is for $R_0^{DT} = 54$ Å. This result agrees well with the spectral overlap measurement of 56 ± 1 Å. (b) High donor concentration systems. The solid curves through the data were calculated without adjustable parameters using the LAF theory. The agreement is excellent over the MG concentration range and for a variety of other R6G concentrations (not shown).

To further test the validity of the results presented above, we studied the same concentration ranges of R6G and MG using glycerol as the solvent. Glycerol is extremely viscous and on the time scales of interest for these experiments the rates of bulk molecular diffusion and molecular rotation can be taken to be zero. The R6G lifetime τ_D was determined from fluorescence mixing studies of a number of dilute glycerol solutions ($\sim 5 \times 10^{-5}$ M), to be 3.17 ± 0.05 ns. This is in good agreement with a previously reported value of 3.1 ± 0.1 ns.[13] The R_0^{DT} was determined from time resolved donor decays in the Förster limit. The results from the fluorescence mixing studies of the Förster limit are shown in Fig. 4(a). They yield $R_0^{DT} = 54 \pm 1$ Å, while transient grating and probe pulse experiments found $R_0^{DT} = 54 \pm 2$ and 55 ± 2 Å, respectively. The measured R_0^{DT} of 54 ± 1 Å is in good agreement with a previous time resolved

measurement of 53 ± 1 Å made by Rehm and Eisenthal,[8] and with our spectral overlap measurement of 56 ± 1 Å.

R_0^{DD} has been previously measured in glycerol, using the same time resolved fluorescence mixing technique, in a study of donor–donor energy transport induced fluorescence depolarization.[13] Molecular rotation prevents similar experiments in ethanol. The fluorescence mixing experiment gave a value of 50 ± 2 Å which compares favorably with a recent spectroscopic determination of 52 ± 1 Å.[26]

The fluorescence mixing results for R6G-MG glycerol solutions ($C_D \sim 1$) are shown in Fig. 4(b). The solid curves are again calculated from Eq. (5) with the constants $\tau_D = 3.17$ ns, $R_0^{DT} = 54$ Å, $R_0^{DD} = 50$ Å, $\gamma = 0.846$, $\alpha = 0.247$, and $\beta = 0.558$. The experiments and theory are compared with no adjustable parameters. Agreement similar to that displayed in Fig. 4(b) was also found for other donor concentrations, i.e., $C_D = 0.7$ (2×10^{-3} M) and $C_D = 0.3$ (1×10^{-3} M). The close agreement between experiments and theory for the R6G and MG mixtures in glycerol solvent is further support for the applicability of LAF theory to transport and trapping in this type of system and confirms the validity of neglecting the effects of bulk molecular diffusion and the deviation of γ from unity in experiments using ethanol as the solvent.

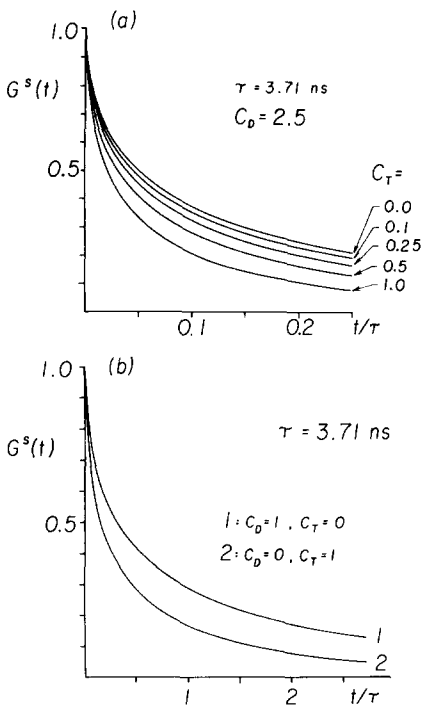

FIG. 5. (a) $G^s(t)$, the probability of an excitation being found on the originally excited donor molecule calculated using the LAF theory for R6G-MG systems. (The decay due to R6G excited state lifetime has been removed from the calculation to more clearly illustrate transport effects.) The loss of excitation probability from the original molecule is dominated by donor–donor transport until the trap concentration becomes comparable to the donor concentration, i.e., $C_T \sim 1$. (b) An illustration of the importance of back transfer in excited state transport dynamics. The upper curve involves donor–donor transport only ($C_D = 1$, $C_T = 0$). Back transfer tends to maintain probability on the initially excited molecule. The lower curve involves donor to trap transport only ($C_D = 0$, $C_T = 1$) for which there is no back transfer, and therefore $G^s(t)$ decays faster even though the overall reduced concentration ($C = 1$) is the same for the two curves.

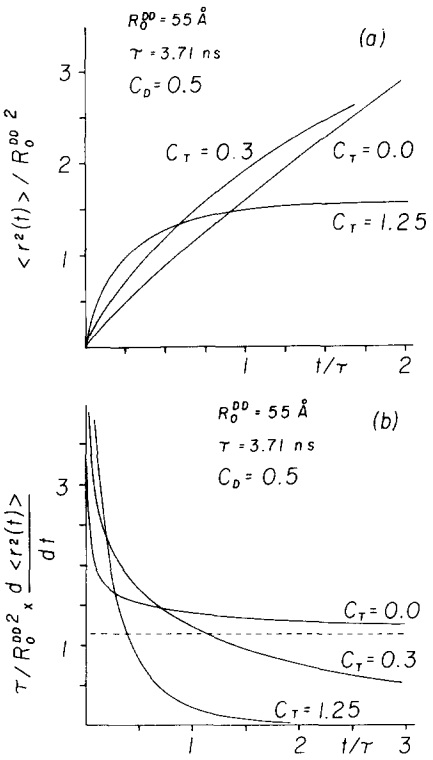

FIG. 6. (a) Theoretically calculated mean-square-displacements of the excitation for the R6G-MG ethanol system using the LAF theory (two-body approximation Ref. 15). Lifetime decay is not included. These curves, for a fixed donor concentration ($C_D = 0.5$), demonstrate the effect of trapping on the MSD. The curve with $C_T = 0.0$ gives the MSD in the absence of trapping. When $C_T \neq 0$, the MSD initially increases faster because of the lack of back transfer from traps. However, at longer times the MSD for a system with traps reaches a finite limit as the excitations become immobilized on traps. (b) The time derivatives of the MSD curves of (a). If the excitation trasport is diffusive, the time derivative is a horizontal line $6D$ where D is the diffusion constant. The $C_T = 0.0$ curve indicates nondiffusive behavior in the absence of trapping. The curve asymptotically approaches the diffusive limit (dashed line) at long time. The curves with $C_T \neq 0$ asymptotically approach zero at long time, i.e., transport comes to a halt.

V. EXCITED STATE TRANSPORT DYNAMICS IN RHODAMINE 6G-MALACHITE GREEN SYSTEMS

The transport and trapping experiments described above are directly related to the time evolution of the Green function solution to the system's master equation. The close agreement between experiment and theory demonstrates that the LAF diagrammatic procedure yields an excellent approximation to the Green function. This knowledge of the Green function permits any property of the transport system to be calculated. To provide a better picture of excited state transport in the R6G-MG systems, three of the important time dependent parameters are displayed in Figs. 5 and 6.

The curves were calculated using the constants of the R6G-MG ethanol solutions determined experimentally above.

Figure 5(a) shows calculations of $G^s(t)$ for a donor concentration of $C_D = 2.5$, and various trap MG concentrations ranging from $C_T = 0$ to $C_T = 1.0$. $G^s(t)$, the probability of finding the initially excited molecule still excited at the time t is an important physical property of the system. It is also central in the theoretical treatment as can be seen from Eq. (1) for $G^D(\mathbf{k}, \epsilon)$. $G^s(t)$ would decay even in the absence of transport due to the excited state lifetime. To illustrate the transport properties of the system, the effect of lifetime has been removed from $G^s(t)$, i.e., the $G^s(t)$ plotted, is the loss of probability from the initial molecule because of excited state transport only. As the trap concentration is increased, $G^s(t)$ decreases more rapidly. Traps have an effect on $G^s(t)$ which is disproportionate to their number when compared to the donor concentration. As the donor concentration is increased, $G^s(t)$ will decay more rapidly because there is an increased rate of leaving the initial molecule. However, transfer away from the initial donor to another donor provides the opportunity for back transfer. Back transfer helps maintain probability on the initial molecule, i.e., back transfer decreases the rate of fall of $G^s(t)$. In contrast, transfer to a trap prevents further transport and eliminates the possibility for back transfer, resulting in traps having a greater effect on $G^s(t)$ than donors. This is demonstrated in Fig. 5(b) where the reduced trap concentration, $C_T = 1$, is shown to deplete probability on the initially excited molecule much more rapidly than an identical reduced donor concentration, $C_D = 1$.

Figure 6(a) shows calculations of $\langle r^2(t)\rangle$, the ensemble average mean-square-displacement (MSD) of the excitation in a solution of R6G donors, with and without MG traps. Again to emphasize the time dependent transport properties, the effect of lifetime has been eliminated. The curve for donor–donor transport in the absence of traps ($C_T = 0$) is not linear, i.e., the MSD is not increasing linearly with time. Thus excited state transport, although incoherent (hopping transport), is not classically diffusive in the sense that the MSD is not given by a constant ($6D$, where D is the diffusion constant) multiplied by time. As time increases, the transport approaches diffusive behavior. This can be seen more clearly from the time derivative of the MSD shown in Fig. 6(b). The MSD for systems with traps ($C_T \neq 0$) does not increase indefinitely, but approaches a finite value as all of the excitations become trapped and therefore immobile. However, it is interesting to note that the MSD for systems with traps actually increases faster at very short time than the system for which $C_T = 0$. As discussed in connection with $G^s(t)$, this is because the traps inhibit back transfer. The initial rate of increase of the MSD is somewhat slowed by the back transfer, and therefore systems with traps initially have a faster increase in the MSD. However, at longer times traps prevent continued transport, and systems with $C_T = 0$ will have a greater MSD.

Figure 6(b) shows the time derivatives of the MSD, $d[\langle r^2(t)\rangle]/dt$, for the curves displayed in Fig. 6(a). For $C_T = 0$, the derivative becomes constant as time increases. The dashed line indicates the theoretically calculated constant, which is $6D$. Thus at short times transport is not diffusive, but becomes diffusive at long times. Low donor concentration samples ($C_D < 1$, $C_T = 0$) require many excited state lifetimes to reach diffusive limit and therefore transport is effectively nondiffusive. For systems with $C_T \neq 0$ transport does not become diffusive at any time. As time increases, the derivative goes to zero, i.e., the MSD becomes a constant independent of time. For a given C_D, the cessation of transport occurs at earlier times as C_T increases.

ACKNOWLEDGMENTS

We would like to thank Roger F. Loring for very helpful conversations relating to the theoretical aspects of this work and for use of his computer programs in calculating the theoretical curves. We would also like to thank M. D. Ediger and R. S. Moog for their aid in the determination of R_0^{DT}. RJDM would like to thank the Natural Sciences and Research Council of Canada for a postgraduate scholarship. MP would like to acknowledge a USA–France exchange postdoctoral fellowship. This work was supported by the Department of Energy, Office of Basic Energy Sciences (Grant DE-AT03-82ER12055), and the National Science Foundation, Division of Materials Research (Grant DMR 79-20380).

[1](a) S. J. Vavilov, Z. Phys. **50**, 52 (1925); (b) J. Perrin, 2nd Conseil de Chimie, Solvay, Bruxelles (1924).
[2]D. L. Dexter, J. Chem. Phys. **21**, 836 (1953).
[3]N. J. Turro, *Modern Molecular Photochemistry* (Benjamin/Cummings, New York, 1978).
[4](a) R. W. Olson, Roger F. Loring, and M. D. Fayer, Appl. Opt. **20**, 2934 (1981); (b) W. H. Weber and J. Lambe, *ibid.* **15**, 2299 (1976); (c) J. S. Batchelder, A. H. Zewail, and T. Cole, *ibid.* **18**, 3090 (1979).
[5](a) R. M. Pearlstein, Proc. Natl. Acad. Sci. U.S.A. **52**, 824 (1964); (b) T. Markvart, J. Theor. Biol. **72**, 91 (1978); (c) G. Porter, Proc. R. Soc. London Ser. A **362**, 281 (1978).
[6](a) T. Förster, Ann. Phys. Leipzig **2**, 55 (1948); (b) T. Förster, Z. Naturforsch. Teil A **4**, 321 (1949).
[7]S. I. Vavilov and M. D. Galanin, Sov. Phys. Dokl. **67**, 811 (1949).
[8]D. Rehm and K. B. Eisenthal, Chem. Phys. Lett. **9**, 387 (1971) and references therein.
[9]D. P. Millar, R. J. Robbins, and A. H. Zewail, J. Chem. Phys. **75**, 3649 (1981).
[10](a) W. Klöpffer, Ann. N. Y. Acad. Sci. **366**, 373 (1981); (b) C. W. Frank, and L. A. Harrah, J. Chem. Phys. **61**, 1526 (1974).
[11](a) P. M. Selzer, D. S. Hamilton, and W. M. Yen, Phys. Rev. Lett. **38**, 858 (1977); (b) G. F. Imbusch, Phys. Rev. **153**, 326 (1967).
[12]D. R. Lutz, K. A. Nelson, C. R. Gochanour, and M. D. Fayer, Chem. Phys. **58**, 325 (1981).
[13]C. R. Gochanour and M. D. Fayer, J. Phys. Chem. **85**, 1989 (1981).
[14]H. Scher, S. Alexander, and E. W. Montroll, Proc. Natl. Acad. Sci. U.S.A. **77**, 3758 (1980).

[15]R. F. Loring, H. C. Andersen, and M. D. Fayer, J. Chem. Phys. **76**, 2015 (1982).
[16]S. W. Haan and R. Zwanzig, J. Chem. Phys. **68**, 1879 (1978).
[17]C. R. Gochanour, H. C. Andersen, and M. D. Fayer, J. Chem. Phys. **70**, 4254 (1979).
[18](a) K. Godzik and J. Jortner, J. Chem. Phys. **72**, 4471 (1980); (b) J. Klafter and R. Silbey, *ibid.* 72, 843 (1980).
[19](a) D. L. Huber, Phys. Rev. B **20**, 2307 (1979); (b) D. L. Huber, *ibid.* B **20**, 5333 (1979).
[20](a) R. S. Moog, M. D. Ediger, S. G. Boxer, and M. D. Fayer, J. Phys. Chem. **86**, 4694 (1982); (b) G. Porter, P. J. Sadkowski, and C. J. Tredwell, Chem. Phys. Lett. **49**, 416 (1977).
[21](a) H. J. Eichler, Opt. Acta **24**, 631 (1977); (b) M. D. Fayer, Annu. Rev. Phys. Chem. **33**, 63 (1982).
[22]J. N. Demas and G. A. Crosby, J. Phys. Chem. **75**, 991 (1971).
[23]M. D. Ediger, R. S. Moog, S. G. Boxer, and M. D. Fayer, Chem. Phys. Lett. **88**, 123 (1982).
[24]D. D. Dlott, Ph.D. thesis, Stanford University, 1979.
[25]G. Porter and C. J. Tredwell, Chem. Phys. Lett. **56**, 278 (1978).
[26]M. D. Ediger and R. S. Moog (unpublished).
[27](a) R. J. D. Miller, R. Caselegno, K. A. Nelson, and M. D. Fayer, Chem. Phys. **72**, 371 (1982); (b) K. A. Nelson, R. J. D. Miller, D. R. Lutz, and M. D. Fayer, J. Appl. Phys. **53**, 1144 (1982).
[28](a) M. Yokota and O. Tanimoto, J. Phys. Soc. Jpn. **22**, 779 (1967); (b) U. Gösele, M. Hauser, U. K. A. Klein, and R. Frey, Chem. Phys. Lett. **34**, 519 (1975); (c) U. K. A. Klein, R. Frey, M. Hauser, and U. Gösele, Chem. Phys. Lett. **41**, 139 (1976); (d) R. A. Auerbach, G. W. Robinson, and R. Zwanzig, J. Chem. Phys. **72**, 3528 (1980).
[29]A. Einstein, *Investigations on the Theory of Brownian Movement* (Dover, New York, 1956).
[30]C. Bojarski and J. Dudkiewicz, Chem. Phys. Lett. **67**, 450 (1979).